Nuclear Instruments and Methods in Physics Research A 385 (1997) 339–344

ELSEVIER

NUCLEAR INSTRUMENTS & METHODS IN PHYSICS RESEARCH Section A

Spallation neutron spectra measurements Part I: Time-of-flight technique

F. Borne [a,*], S. Crespin [a], S. Leray [b,c], Y. Patin [a], M. Beau [a], A. Boudard [c], F. Boué [a], P. Bouyer [b], J.L. Boyard [b], F. Brochard [b], D. Drake [a], J.C. Duchazeaubeneix [b], J.M. Durand [b] J. Fréhaut [a], L. Kowalski [f], R. Legrain [c], J.P. Lochard [a], E. Martinez [a], S. Ménard [d], G. Milleret [b], E. Petibon [a], F. Plouin [b], Y. Terrien [c], J. Thun [b,e], M. Uematsu [b], S. Vuillier [c], D.M. Whittal [b]

[a] *DPTA/SPN, CEA Bruyères-le-Châtel, France*
[b] *Laboratoire National SATURNE, Saclay, France*
[c] *DAPNIA/SPhN, Saclay, France*
[d] *IPN, Orsay, France*
[e] *Uppsala University, Uppsala, Sweden*
[f] *Montclair State University, USA*

Received 2 September 1996

Abstract

We present an experimental method based on a time-of-flight technique between the tagged incident particles and a thick liquid NE213 scintillator to measure neutron energy spectra from 3 to 400 MeV at the Saturne synchrotron of Saclay. Efficiency measurements are made using a pulsed neutron source from the Tandem Van de Graaff of Bruyères-le-Châtel at low energies and a quasi-monoenergetic neutron beam at Saturne up to 50 MeV.

PACS: 25.40.Sc; 07.07.-a; 29.40.Mc

1. Introduction

Part I and Part II of this paper are devoted to experimental techniques to measure neutron energy spectra between 3 and 1600 MeV. The primary aim of the study is to obtain reliable neutron production cross sections for the spallation process induced by protons and deuterons between 800 and 1600 MeV. These experiments are being performed at the synchrotron of the Laboratoire National Saturne (LNS) which delivers a beam without RF structure. This makes the use of the conventional time-of-flight technique impossible [1].

Two different experimental techniques are used. Low energy neutrons are measured using the time-of-flight between the tagged beam particles and the neutrons detected in a thick liquid scintillator. This technique described in the present paper (Part I) is limited to about 400 MeV. The high energy neutrons are measured with a liquid hydrogen converter and a magnetic spectrometer and will be described in the following paper (Part II) [2].

The paper is organized as follows: In Section 2 we describe the experimental technique and setup. Section 3 is devoted to the electronics and data acquisition. The Neutron-Gamma discrimination is also presented. The off-line data analysis for spallation results is outlined in Section 4. In Section 5 we explain how the neutron detector efficiency curve is obtained for a given energy threshold and other experimental parameters. An example of a spallation neutron spectrum obtained is shown in Section 6.

2. Experimental method

For the low energy experimental arrangement described here (see Fig. 1), the proton beam is focused through a 1 mm thick plastic scintillator (smaller than the targets), called SC, onto targets of diameter 30 mm. Target length (10 to 36 mm) is chosen as a compromise between energy loss and neutron production rate. The diameter of SC (∅: 28 mm) is made slightly smaller than the diameter of the targets to ensure that all tagged particles subsequently strike the target. The pulses from SC measure the beam intensity and serve as the stop pulse for the time-of-flight measurement. The beam

* Corresponding author. Tel +33 1 69 26 68 31, fax +33 1 69 26 70 63, e-mail borne@bruyeres.cea.fr.

PII S0168-9002(96)01156-4

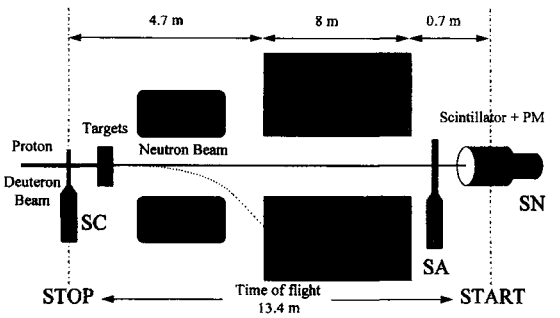

Fig. 1. Low energy experimental setup.

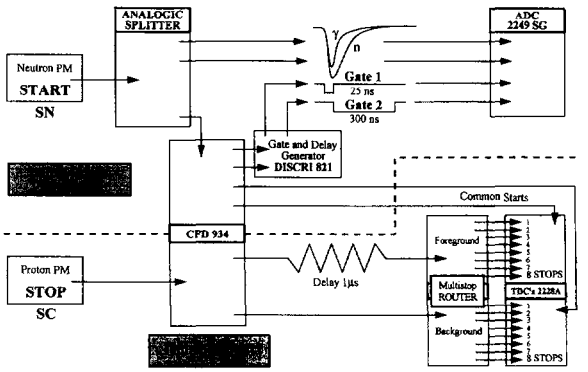

Fig. 2. Low energy electronic setup.

intensity is reduced by machine tuning and slits so that the average counting rate in SC is less than a few 10^6 s^{-1}. At this low intensity the extraction technique introduces some structure in the beam time profile making the instantaneous counting rate somewhat higher than the computed average. Protons that do not interact in the target and other charged particles emitted in the forward direction are swept from the flight path by a magnet called MIMOSA located about 50 cm downstream of the target. The neutrons pass through an 8-m cylindrical collimator of iron-loaded concrete with an exit diameter of 168 mm.

The neutron counter, called SN, is a cylinder with diameter of 127 mm and a length of 178 mm, filled with NE213 liquid scintillator and coupled to a 127 mm diameter photomultiplier. The solid angle subtended by SN, for a distance between SC and SN of 13.40 m, is 0.072 msr at 0°. A 13 mm thick lead sleeve with an outer diameter of 188 mm and a length of 250 mm surrounds the detector and serves as a shield against ambient gamma rays.

A 3 mm thick plastic scintillator-photomultiplier combination, called SA, is placed just in front of SN to detect charged particles.

A 1 m tungsten shadow bar placed between MIMOSA and the collimator can be positioned by remote control in the flight path to absorb target neutrons that would normally have hit SN directly. Its shape is such that neutrons from the target can still hit the collimator wall even with the shadow bar in place. Thus the shadow bar effectively measures the background produced by the collimator. With the shadow bar in place, the difference between target in and target out spectra is found to be small ($\leq 1\%$) so the shadow bar is not used for all of the various target-energy combinations.

Data are taken in different configurations (target in, target out, with and without shadow bar) so that reasonable estimates of the background can be made.

3. Electronics and data acquisition

The pulse-shape technique is used for neutron–gamma discrimination. Fig. 2 shows the electronic arrangement including time-of-flight and neutron–gamma discrimination.

Pulses produced by the neutron detector, SN, are sent to an analogue splitter with three outputs. One of these is used through a CFD as a start pulse for the time of flight measurements and the other two are used in a neutron–gamma discrimination scheme. The discrimination scheme used for data analysis is based on sampling the early portion of the pulse and comparing its charge in a gate of 25 ns to the charge integral of the portion of the pulse that remains after the initial 50 ns. The integral gate is 300 ns long. These signals are analyzed by charge ADCs.

A multistop technique is used taking the stop pulses from SC. They are delayed by one microsecond and sent to TDCs which are used in common start mode with a time range of 1 μs. Our time analysis condition leads to a high probability for the occurrence of several stop pulses for each SN start. In order to make sure the one correlated with the neutron pulse is registered, the train of stop pulses is routed through a pulse separator. The separator accepts a series of pulses and routes each one in turn to separate outputs. These stop pulses are sent to the eight TDCs. The sum of the eight calibrated time

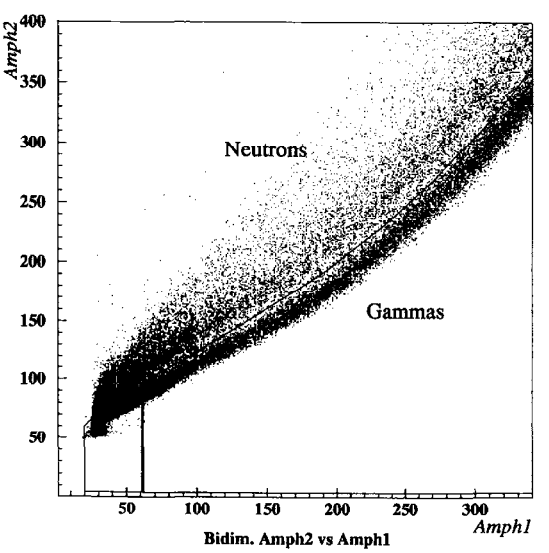

Fig. 3. Typical two dimensional neutron–gamma discrimination plot with two gamma-ray cuts.

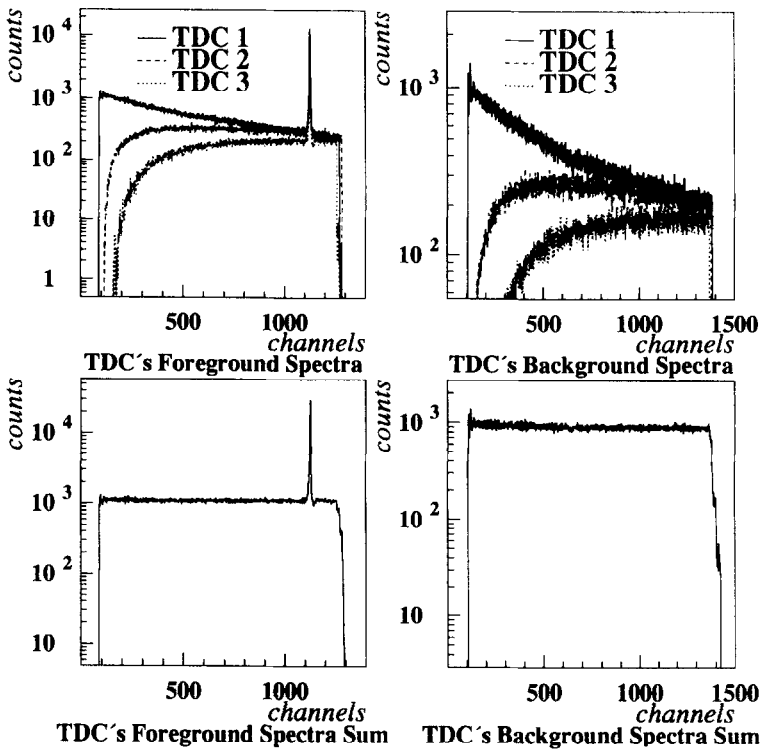

Fig. 4. Individual TDC spectra (limited to the first three for clarity) and the sum of the eight TDCs for both the foreground and background measurements induced by a 1600 MeV deuteron beam on a beryllium target.

spectra gives the correct time of flight spectrum including true and random events. An identical TDC-separator system is used to record the uncorrelated background using non-delayed stop pulses.

The coincidence between SA and SN is recorded as a narrow peak in another TDC and is used as an off line cut to remove these charged particles.

Data are taken in event mode and stored on disk for detailed analysis off line. For each event we have burst number, two amplitudes, sixteen TDCs (eight foreground, eight uncorrelated background) and finally the charged particle rejection arrays. An appropriate set of scalers is also recorded for each burst. They are used mainly to monitor the beam intensity and to evaluate the dead time correction.

4. Sample data analysis

The utility program PAW [3] is used to analyze the data. First, the gamma-ray pulses and charged particles are removed from all time-of-flight spectra. Cuts on the two dimensional arrays of pulse-shape versus energy are employed to eliminate the gamma rays (85% of events) from the time of flight spectra. Fig. 3 displays a typical two dimensional neutron–gamma discrimination plot with associated gamma-ray cuts. The gamma rejection is 95%. The charged particle rejection is quantified as a contribution of 1% of the total spectrum.

Each set of time histograms (foreground and background) was summed and because they did not have exactly the same time calibration or zero time channel, they were aligned and compressed so that each channel corresponded to one nanosecond.

As an example, Fig. 4 shows the time spectra (limited to the first three for clarity) and the sum of the eight for both the foreground and background encoders obtained with 1.6 GeV deuteron beam on a beryllium target to produce monoenergetic neutrons of 800 MeV.

Theoretically, we have a spectrum and a flat random background. Unfortunately a detection dead time (20 ns) on SC introduces a small loss of counting. In order to correct for this, we have made a Monte Carlo simulation taking into account the instantaneous counting rate and the dead time of 20 ns due to SC. This correction is less than 3%. Fig. 5 shows the corrected time of flight spectrum (sum of the eight) with a flat random background for the efficiency measurement with an incident deuteron beam of 1.6 GeV.

Because each time of flight spectrum collected for the efficiency runs consists of a well defined neutron peak with a flat background, it is necessary only to find the area of this peak and to combine it with the target thickness, beam intensity and d + Be differential cross section at 0° to obtain the detection efficiency.

Fig. 6 shows typical corrected time of flight spectra for

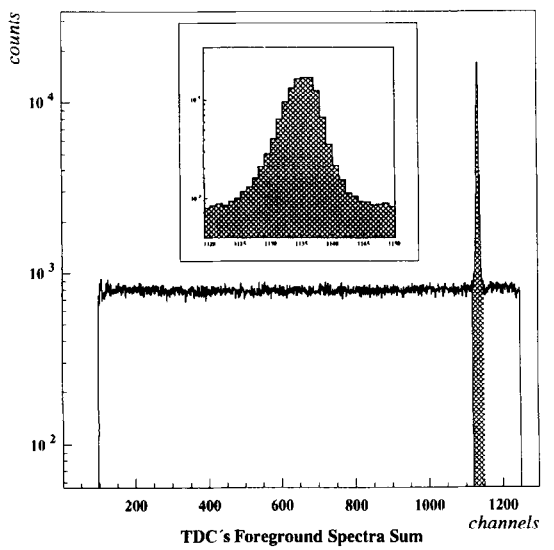

Fig. 5. Corrected TDC foreground spectra (sum of eight) induced by a 1600 MeV deuteron beam on a beryllium target. The inside figure is an enlargement of the "Monoenergetic" neutron peak centered at 800 MeV.

800 MeV protons on a lead target from which the spallation cross section spectrum is extracted by subtracting a flat background from the foreground spectrum.

Folding the time-of-flight spectra to energy spectra tends to produce many data points with poor statistical quality in the lower energy part of the spectra. To avoid this problem, we choose predetermined energy intervals, sum the foreground pulses in each one, and subtract corresponding background sums and divided the result by the energy interval. The resulting spectra (counts/MeV versus energy) are then divided by neutron detection efficiency (see Section 5), number of beam particles, solid angle, and density to obtain cross sections.

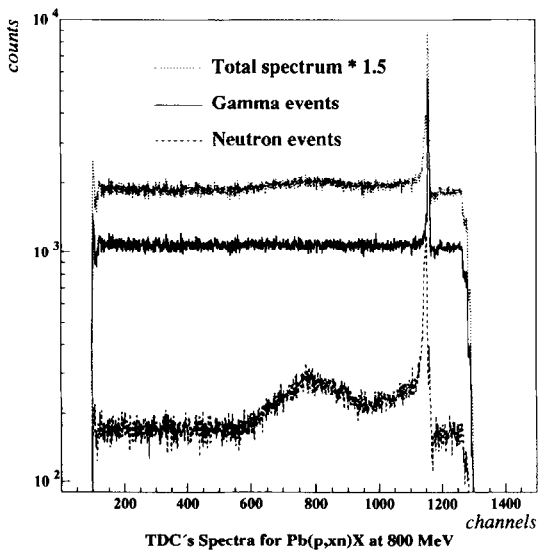

Fig. 6. Typical time of flight spectra for 800 MeV protons on a lead target. The charged particle spectrum is not plotted because of the very low rate ($\leq$1%).

5. Neutron detection efficiency

A pulsed beam from the Centre d'Etudes de Bruyères-le-Châtel's Tandem Van de Graaff is used to measure the efficiency of SN at low energies. Measurements at 2, 3, 5 and 16 MeV are made using the ^{3}H(p,n)^{3}He and the ^{3}H(d,n)^{4}He reactions. A smaller neutron detector (NE213 2-in. $\times$ 2-in.) of known efficiency [4], is used as a reference monitor. It is placed at 20° symmetrically to SN with respect to the beam. At each energy, relative counting rates and solid angles are used to deduce the efficiency of SN. The pulse height bias for the time of flight measurements and the neutron–gamma discrimination scheme is set to 450 keV_{ee} according to the energy calibration using the two gamma rays of an ^{88}Y source. The neutron energy threshold, experimentally deduced, is in this case 3 MeV.

At higher energies the efficiency is measured during the neutron production experiment using a deuteron beam on a beryllium target, with the same experimental arrangement that is used to collect the neutron cross section data. For these measurements, deuteron beams with energies of 100, 200, 400, 800, 1200, and 1600 MeV are used with beryllium targets of thicknesses 3, 25, or 75 mm to produce 0° "monoenergetic" beams of neutrons with energies equal to half that of the incident deuteron energy. The d + Be differential cross section at zero degrees for this breakup (stripping and dissociation) reaction based on the datum from reference [5] is known to within ±20%. The differential cross section values have been extrapolated from Ref. [6] down to 40 MeV, and are shown in Table 1. At low energies the Fermi motion and the energy loss in the target introduce a significant neutron energy spread and thus a larger uncertainty in the breakup cross section.

Fig. 7 displays the measured efficiency of SN as a function of incident neutron energy. For comparison, efficiency points computed using the O5S [7] and KSU [8] codes are also reported. The error bars plotted on the efficiency curve take into account the errors on statistics, the deuteron cross section for stripping and dissociation at zero degrees

Table 1
Stripping and dissociation differential cross sections on beryllium at 0°, used for the efficiency points

Neutron energies [MeV]	$\left(\frac{d\sigma}{d\Omega}\right)_{0°}$ [b/sr]
42	1.04
100	2.56
200	5.38
400	11.79
600	19.24
800	27.73

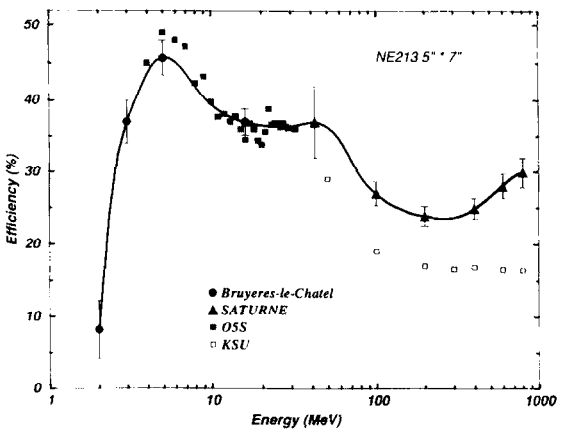

Fig. 7. Detector efficiency vs neutron energy for 450 keV_{ee} bias setting. The circles are measured at Bruyères-le-Châtel Laboratory. The triangles are measured at Laboratoire National Saturne. For comparison efficiency points computed using Monte Carlo O5S [7] (filled squares) and KSU [8] (empty squares) codes are plotted. The solid line is a guide for the eye and is used as the basis for the spallation neutron spectra analysis. The error bar at 42 MeV reflects the effect of the Fermi motion and energy losses in the target.

Table 2
Relative contribution of the lead shield to SN efficiency

Energies [MeV]	TIERCE calculations	Experimental results
200	12%	
400	18%	
600	23%	20%
800	27%	24%

and the solid angle. Above 200 MeV the effect of the lead shield surrounding SN becomes significant and has been estimated by TIERCE [1] [9] calculations. It increases the efficiency by sizeable re-emission of particles towards the SN detector. Table 2 shows the results of these calculations in terms of the relative contribution to the efficiency from 200 to 800 MeV. Two points at 600 and 800 MeV are compared to our experimental results obtained with and without surrounding lead shield. The pion contribution in these results is less than 3% above 400 MeV.

6. Spallation neutron spectrum

Fig. 8 shows a spallation neutron spectrum for a 20 mm long lead target with 800 MeV incident protons as an example of the type of results we have obtained. This figure also presents the high energy portion obtained with the recoil proton spectrometer technique described in the following paper. The agreement between these two methods is better than 15%. The vertical error bars plotted are statistical, the horizontal ones in the time-of-flight measurements represent the FWHM energy resolution at representative neutron energies summarized in Table 3.

[1] This set of codes contains, amongst other things, the HETC developed at Bruyères-le-Châtel from the public version [10] and MCNP [11].

Table 3
FWHM energy resolution. This time-of-flight resolution corresponds to a time resolution of 4 ns

Energies [MeV]	Energy resolution [MeV]
10	±0.2
50	±1.5
100	±4
200	±15
400	±42

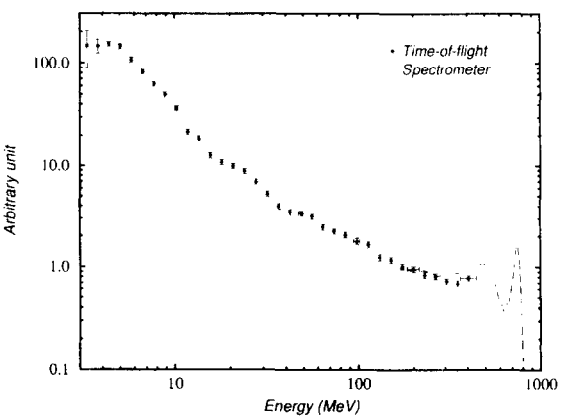

Fig. 8. Experimental (p,xn) spectrum for a ^{208}Pb target with 800 MeV protons. The dotted points are time-of-flight results. Vertical error bars are statistical. For selected points summarized in Table 3 the horizontal error bars represent the resolution. The solid line is obtained with the proton recoil spectrometer technique describe in the following paper [2].

Cross section results of both the high and low energy neutrons for several targets (lead, aluminium, iron, zirconium, tungsten and thorium) and various energies (800, 1200, and 1600 MeV) will be combined and published later.

7. Conclusion

We have developed an experimental method based on a beam-tagging and time-of-flight technique to obtain neutron energy measurements from 3 to 400 MeV. The efficiency of the detector has been directly measured with neutrons of known energies over the full detection range. This experimental method is being used at Saturne together with the method described in the following paper [2]. These two methods are devoted to measure high energy neutrons in the study of spallation neutron production between 800 and 1600 MeV on various targets.

References

[1] S. Cierjacks, Y. Hino, F. Raupp, L. Buth, D. Filges, P. Cloth and T.W. Armstrong, Phys. Rev. C 36 (1987) 1976.

[2] E. Martinez et al., this issue, Nucl. Instr. and Meth. A 385 (1997) 345.
[3] PAW Physics Analysis Workstation, CERN Program Library (unpublished).
[4] G. Grenier, Bulletin BNM 37 (July 1979).
[5] G. Bizard, F. Bonthonneau, J.L. Laville, F. Lefebvres, J.C. Malherbe, R. Regimbart, J. Duflo and F. Plouin, Nucl. Instr. and Meth. 111 (1973) 445.
[6] G. Bizard, F. Bonthonneau, J.L. Laville, F. Lefebvres, J.C. Malherbe, R. Regimbart, J. Duflo and F. Plouin, Nucl. Instr. and Meth. 111 (1973) 451.
[7] R.E. Textor and V.V. Verbinski, ORNL 4160 Oak Ridge National Laboratory (1968).
[8] R.A. Cecil, B.D. Anderson and R. Madey, Nucl. Instr. and Meth. 161 (1979) 439.
[9] O. Bersillon, private communication (1995).
[10] T.W. Armstrong and K.C. Chandler, Nucl. Sci. Eng. 49 (1972) 110.
[11] J. Briesmeister (ed.), LA-12625-M, Los Alamos National Laboratory (1993).